R.Revathi* et al.
(IJITR) INTERNATIONAL JOURNAL OF INNOVATIVE TECHNOLOGY AND RESEARCH
Volume No.2, Issue No. 4, June – July 2014, 1017 – 1022.

Research Article

Observations of Seismo-Ionospheric Perturbations Using Wavelet Analysis

R.REVATHI
Women Scientist
Dept. of ECE
K L University, Guntur, A.P. India.

K.S.RAMESH
Professor
Dept. of ECE
K L University, Guntur, A.P. India.

M.VENU GOPAL RAO
Professor
Dept. of ECE
K L University, Guntur, A.P. India.

G. RAMA SRI CHAITANYA
B.tech student
Dept. of ECE
K L University, Guntur, A.P. India.

A.JASMITHA
B.tech student
Dept. of ECE
K L University, Guntur, A.P. India.

G.TEJASWI
B.tech student
Dept. of ECE
K L University, Guntur, A.P. India.

A.VIJAYA REKHA
B.tech student
Dept. of ECE
K L University, Guntur, A.P. India.

Abstract: **Electromagnetic signals generated before and during the Earthquakes lie in a broad range of frequencies from MHz to Qasi DC frequencies (Darcy Karakelian et.,al 2000[1]). These signals reach higher altitudes and perturb the background atmosphere by dumping their energy (V.V. Hegai et.,al 2006[2] , Tadahiko Ogawa et.,al 2012[3]). These electromagnetic signals cause perturbations in the ion content of the ionosphere. The study of these perturbations is important to understand their evolution mechanisms. The ionospheric variability is measured in terms of ionospheric Total Electron content (TEC). The complex time varying and non-linear characteristics of Seismo-ionospheric perturbations are different from other disturbances (Li-ming He et.,al, 2011[4]). The earthquake which occurred in Indonesian region on 1st Sepember 2013 with a magnitude M>6 is considered for the present study. The time frequency analysis of narrow transition regions of these signals are analyzed using Wavelets (Gwal A.K., et., al 202[5], Michael E. Contadakis et.,al 2012[6]) . Analysis of the non-stationary data using wavelets provides time localized alternatives and complex wavelets are useful in accurate detection and recognition of transient signals. The results show that these perturbations are observed three days before the Earthquake and are increasing in nature. The observed periodicities on the Earthquake day may represent that there is possible transfer of momentum and energy from lower atmosphere to upper atmosphere.**

Key Words: **Seismo-ionospheric Perturbations, Wavelets, Non-stationary data, Transient analysis.**

I. INTRODUCTION

Ionosphere reacts to wide range of disturbances, such as Solar wind plasma energy particles from Sun, tides, gravity waves and a wide range of electromagnetic waves from below (A. K. Singh et.,al, 2011[7]). The coupling occurs mainly through dynamical, chemical and electrical processes (V.M. Sorokin et.,al 2001[8], Sergey Pulinets 2004[9]). Significant ionospheric perturbations are reported during quiet period of geomagnetic activity and solar activity for many large earthquakes (J. Y. Liu et.,al, 2013[10]). The transient nature of these perturbations disturbs the upper atmosphere resulting in considerable changes in the Total Electron Content (TEC) seen before large earthquakes leading to lithosphere-Troposphere-Ionosphere coupling. (O. Molchanov[11] et.,al 2004, Harrison, R.G, et.,al 2009[12]). The coupling of the lower and upper atmosphere is a well explained phenomena starting from radon gas release (Y. Omori[13] et.,al, 2007, Surinder Singh[14] et.,al 2010), atmospheric ionization leading to latent heat variations and generation of acoustic and atmospheric gravity waves (M. Matsumura[15], et.,al 2011, V.V. Hegai[16], et.,al, 2004). GPS data available worldwide over large networks are analyzed and the TEC variations have been profoundly observed for large seismic events.

International GNSS station (IGS) data near the epicenter, before and during the earthquake is considered and analyzed. The coupling of lower and upper atmosphere during the earthquake results in short time transient signals of varying complex and non linear characteristics. This study will be helpful in realizing the coupling of energy and momentum process from lower atmosphere to upper atmosphere leading identification of possible source mechanisms of these disturbances. Wavelets being an efficient tool in identification of transience in signals are applied on the time series data.

A. Event Considered:

The analysis is done for the large earthquake which occurred in Indonesia on 1 September 2013 having a magnitude of M>6, at 11.52 UTC at (7.440°S, 128.221°E) with a depth of 112.0km (69.6mi). The boundary of the Australian Pacific plate and the east coast of Pupa New Guinea are dominated by the general

Research Article

northward subduction of the Australian plate. Along the south Solomon trench, the Australian plate converges with the Pacific plate at a rate of approximately 95 mm/yr towards the east-northeast. Seismicity along the trench is dominantly related to subduction tectonics and large earthquakes are common.

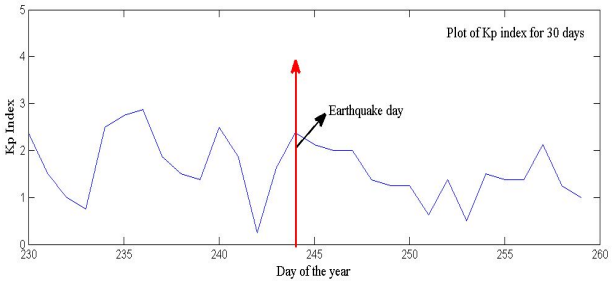

Fig1: Kp Index plot for 230 to 259 GPS days of the year.

To verify whether the observed ionospheric perturbations are caused by the impending earthquake, where Kp index values for the 30 days are plotted considering the earthquake day as the 15th day of the month. It is observed that there is no significant geomagnetic activity 10 days before and after the occurrence of the earthquake as the Kp index value is not more than 3 for all the 30 days. This data is given by World Data Center (WDC) for geomagnetism, Kyoto, Japan.

II. DATA

The Slant Total electron content (STEC) is taken from the IGS station near the epicenter situated at Bakosurtanal, Cibinong, West Java, Indonesia (-6.49°N, 106.85°E) (Cahyadi[17] et.,al 2013). The IGS data comprises of time, PRN number, latitude, longitude, azimuth angle, elevation angle, STEC, Vertical Total electron content (VTEC), etc. Strong variations in STEC are observed in the PRN numbers 4, 18. The PRN number 18 is selected for the study as there are strong variations in STEC 3 days before and during the earthquake. The STEC for the GPS receiver is given by

$$STEC = \left(\frac{1}{40.3}\right) * (f_1 f_2/(f_1 - f_2)) * (P_1 - P_2)$$

The STEC plots for the three days of the year 242, 243 and 244(earthquake day) are as shown.

It is observed that there are significant variations in the STEC plots during the occurrence of the earthquake.

Fig 2: STEC plots for PRN 18 for GPS days 242 day of the year (two days before the earthquake), 243 day of the year (one day before the earthquake) and 244 day of the year (Earthquake day).

A. Methodology:

Wavelets are functions of finite length or fast-decaying oscillations. These are an effective tool for transient signal analysis for representing the functions that have discontinuities and sharp peaks and for accurately

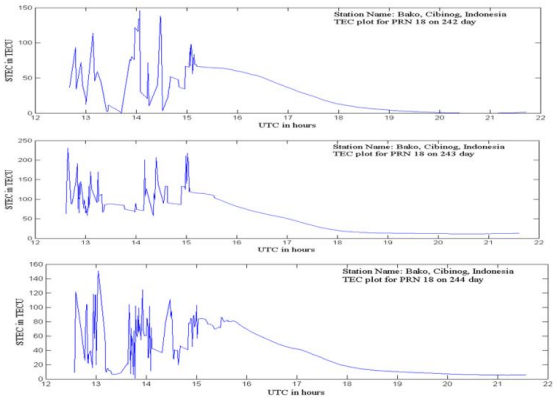

deconstructing and reconstructing finite, non-periodic and non –stationary signals. The frequency range of each scale can be assigned individually. Each scale component is studied with a resolution that matches its frequency.

In the present work Complex Gaussian wavelets and Haar wavelets are used to study the time series data. The wavelet transform equation for STEC is as given below. It is a function constructed from translations and dilations of a of a single function called mother wavelet.

$$\psi_{a,b}=(1/\sqrt{a})\psi(STEC-(b/a))a,b\in\mathcal{R},a\neq 0$$

Analysis of temporal evolution of the frequency content of a given signal or time series data is done using Continuous wavelet transform (CWT). The application of the CWT to two time series and the cross examination of the two decompositions can reveal localized similarities in time and scale (frequency). Areas in the time-frequency plane where two time series exhibit common power or consistent phase behavior indicate a relationship between the signals.

Complex analytical wavelets allow us to draw spectral density of the given data. Complex Gaussian wavelet 2 is used to draw the spectral density of a given time series data. The Complex Gaussian wavelet is the Pth derivative of the integer P.

$$f(STEC) = C_p e^{-iSTEC} e^{-i(STEC)^2}$$

taking the pth derivative of f. The integer p is the parameter of this family and in the previous formula, C_p is such that where $f^{(p)}$ is the pth derivative of f.

$$|f^{(p)}|^2 = 1$$

The Haar wavelet transform for the STEC is given as

$$\psi_{n,k}(\text{STEC}) = 2^{\frac{n}{2}}\psi(2^n\,\text{STEC} - k), t\in\mathcal{R}$$

The periodicities in the variations are studied against a normal STEC in which there are no significant variations. For this PRN 1 on the 244 day(Earthquake day) of the year is considered. Figure 3 represents STEC values in TECU for PRN 1 on 244 day of the year.

Research Article

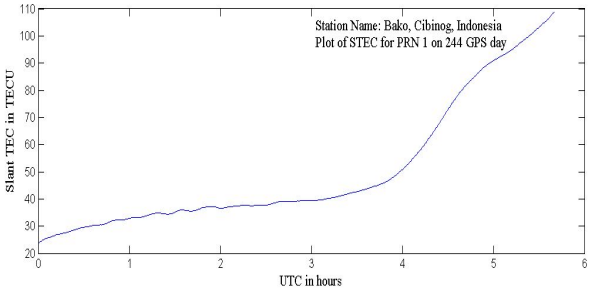

Fig 3: STEC plot for PRN 1 on 244 (earthquake day) day of the year.

III. RESULTS AND DISCUSSION

The Continuous Wavelet Transforms (CWT) are drawn for STEC data on 242 day of the year (two days before the earthquake), 243 day of the year (one day before the earthquake), & 243 day of the year, 244 day the year (earthquake day). Figure 4 represents CWT plot for 242(two days before the earthquake) day of the year and 243(one day before the earthquake) day of the year.

The left side of the Fig 4 represents 242 day of the year and right side represents 243 day of the year. The first row represents STEC perturbations for PRN 18 on 242(two days before the earthquake) and 243(one day before the earthquake) days the year. The second row represents the energy at different scales of frequencies corresponding to perturbations in STEC on both days of the year. The third row represents the phase components at same scales of frequencies where the energy is calculated.

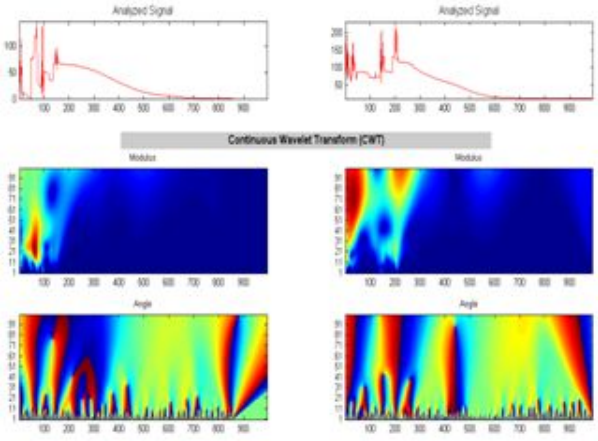

Fig 4: CWT plot for PRN 18 on days 242(two days before the earthquake) and 243(one day before the earthquake).

The energy per unit scale of frequency has increased from 242 day of the year to 243 day of the year. It is clearly observed that on 242 day the energy is concentrated on scales 11 to 31 and for 243 day the energy has concentrated from scales 31 to 91. All these plots are drawn for the same time scale of STEC (starting from 12 to 22 hours UTC) representing the perturbations in the STEC. In the phase angle plot peaks are more dominantly observed on 243 day of the year compared to 242 day of the year.

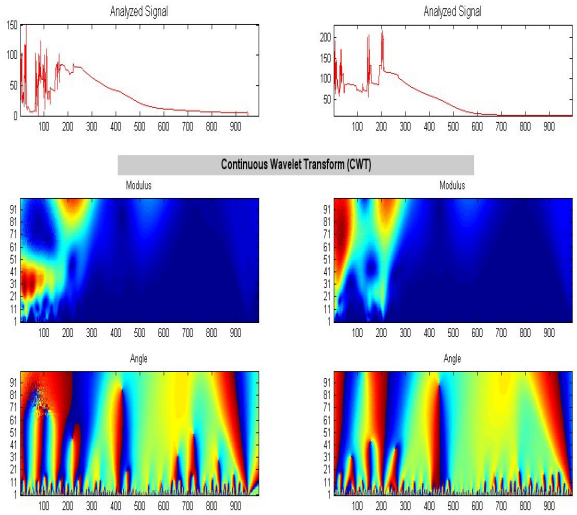

Fig5: CWT plot for PRN 18 on days 244 (earthquake day)and 243 (one day before the earthquake) .

Figure 5 represents CWT plot for 243 (one day before the earthquake) day of the year and 244(earthquake day) day of the year. The left side represents the 244 day (earthquake day) of the year and the right side represents 243 day of the year (one day before the earthquake).

The first row of figure 5 represents the STEC in TECU on 244(earthquake day) day and 243(one day before the earthquake) day. These are also drawn to same time scale from 12 to 22 hours UTC.

The second row represents the energy plots at different scales of frequency corresponding to the perturbations in STEC. It is observed that the energy has sustained on the earthquake day (244 day of the year). In the phase angle plot of the 244 day of the year (earthquake day) clear peaks are seen representing the periodicities in the STEC.

CWT is also applied to PRN 18 (disturbed STEC) and PRN 1(undisturbed STEC) to verify the similarities in the data on 244 (earthquake day) day of the year. Figure 6 represents the similarities in the STEC for PRN 1 and PRN 18

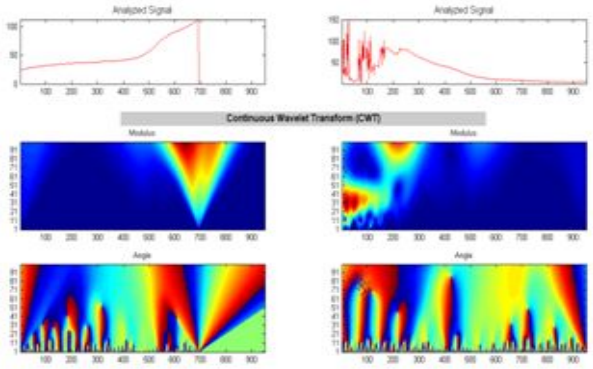

Fig 6: CWT plot for PRN 1 and PRN 18 on 244 day (earthquake day)

Research Article

The left side of the figure represents PRN 1and right side represents PRN 18 for 244 day (earthquake day) of the year. It is clearly observed that the energy (second row) in

STEC of PRN 18 is more strong and sustained than compared to PRN 1.

Is observed in PRN 18, that there is damping phase corresponding to transient nature of the seismo-ionospheric perturbations may be attributed to the possible transfer of energy and momentum due to impending earthquake.

Wave coherence is used to understand the correlation between the given time series data. The wave coherence is plotted for 242 (two days before the earthquake) day of the year and 243(one day before the earthquake) day of the year. (Fig 7)

Figure 7 represents STEC for two PRN's in the first figure, modulus and the relative phase angle plot in the second. In the energy and modulus plot lowest energy points represent the points of disturbance and the arrows represent the relative phase angle difference between the STEC perturbations.

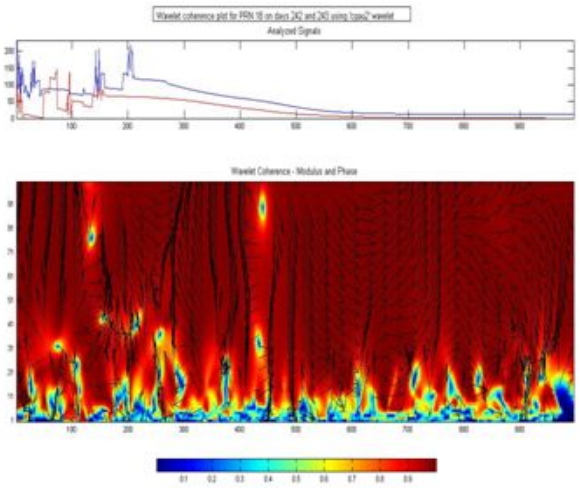

Fig 7: Wave coherence plots for 242 (two days before the earthquake) day of the year and 243(one day before the earthquake) day of the year for PRN 18.

We observe that near the disturbance points the arrows are pointed in all directions representing the distribution of energy. It is also observed that the direction of the arrows at other places is having a sequence order representing a periodic nature.

Figure 8 represents the wave coherence plot for 243(one day before the earthquake) day of the year and 244(earthquake day) day of the year.

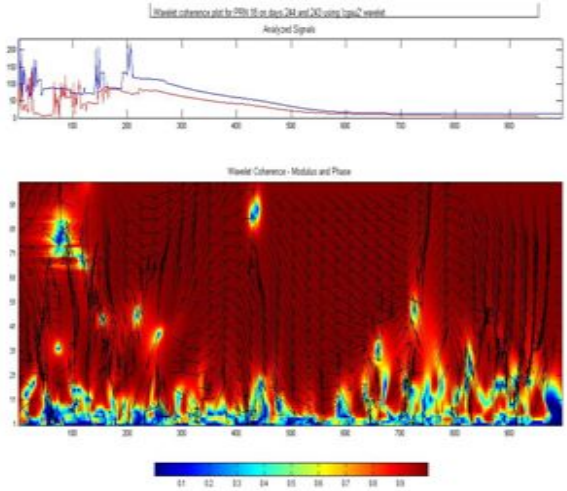

Fig 8: Wave coherence plots for 243(one day before the earthquake) day of the year and 244(earthquake day) day of the year for PRN 18.

It is clearly observed that there is an enhancement in the energy of disturbance. The periodicities in the STEC perturbations are more clearly observed in the direction of the arrows representing the relative phase angle difference for the two days.

The wave coherence plot for PRN 1 and PRN 18 on 244 (earthquake day) day of the year is also drawn to observe the correlation of the energy. Figure 9 represents the wave coherence plot for PRN 1 and PRN 18 on 244 day (earthquake day) of the year and is in good agreement with the above said results.

The relative phase angle difference is either in upward or downward direction.(fig 9) It is not zero at any point in the figure. The disturbed STEC may have changed the direction of the relative phase angle between the two STEC data.

In this analysis Haar wavelets are also used, which shows a clear view of the periodicities present in the STEC perturbations on 244(earthquake day) day of the year.

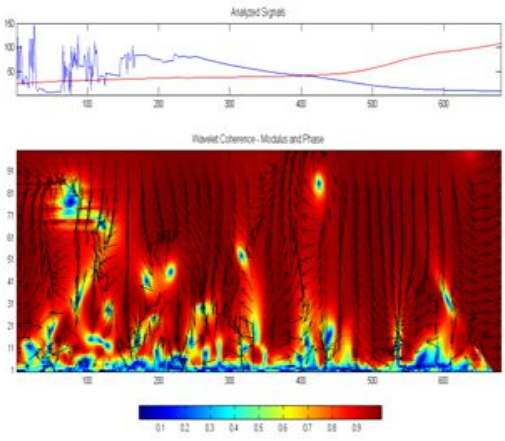

Fig 9: Wave coherence plots for PRN 18 and PRN 1 on 244 (earthquake day) day of the year.

Research Article

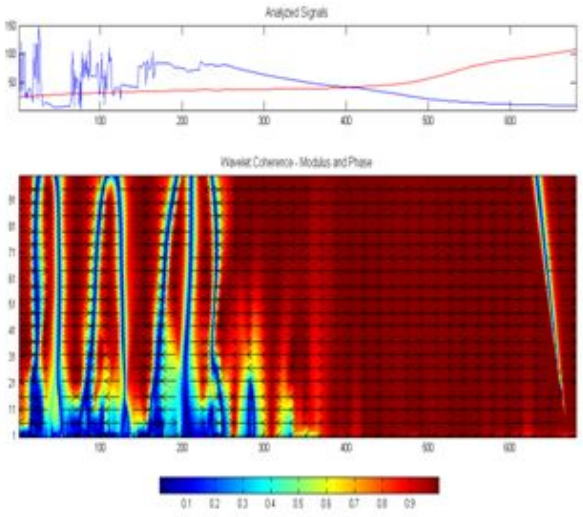

Fig 10: Wave coherence plot using Haar wavelet for PRN for 1 and PRN 18 on 244 (earthquake day) day of the year

In the modulus and phase plot of fig 10 we observe clear periodicities in the energy and the phase of the signal is 180^{o} out of phase at each transition of the energy. This show that there is a possible transfer of energy and momentum may correspond to the impending earthquake. The discontinuities in the STEC are drawn using Haar wavelet for PRN 18 on 242 (two days before the earthquake) day of the year, 243(one day before the earthquake day) day of the year, 244(earthquake day) day of the year and for PRN 1 on 244(earthquake day) day of the year. The discontinuity plot is as given below.

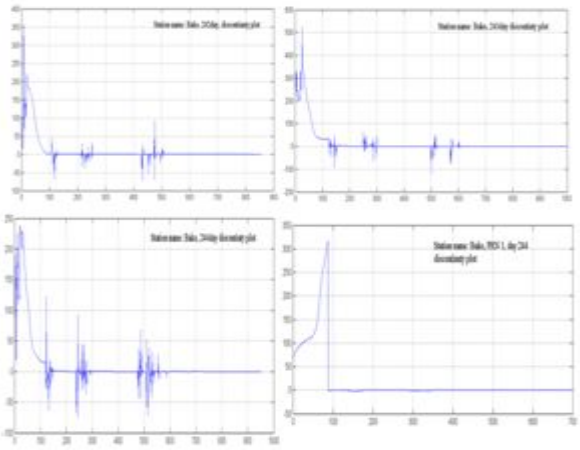

Fig 11: Discontinuity plot for PRN 18 on 242 (two days before the earthquake) day of the year, 243 (one day before the earthquake) day of the year, 244(earthquake day) day of the year and PRN1 on 244 day of the year.

It is clearly seen that the strength of the discontinuities have been increasing form 242 day of the year to 244 day of the year for PRN 18 (starting from the top left) and for PRN 1 the on 244 day of the year there are no discontinues is the STEC plot. This shows that the observed STEC perturbations may corresponds to the impending earthquake.

The ionization of the lower atmosphere at the earthquake preparation zone is a local phenomenon where these changes are observed due to the emission of radon gasses. This shows that we have to consider the TEC variations at a location which is not far away from the epicenter (moderately). Comparison of TEC observations over a wider area may not result in clear understanding of the source mechanisms atleast at low latitudes. An attempt is made in this paper to check whether the observed STEC perturbations correspond to the impending earthquake or not. It is clearly observed that the perturbations are due to the strong earthquake occurred over there.

IV. CONCLUSIONS

The complex time varying and non-stationary time series analysis using Wavelets will bring out the short time transients present in the data. The transient nature of the seismo-ionospheric perturbations was studied using complex wavelets. It reveals that there is transfer of energy and momentum from lower atmosphere to upper atmosphere near the epicenter, starting from two days before the occurrence of the earthquake. The enhancement in the modulus and phase of the perturbations has been clearly observed two days before the earthquake. The attempt in this direction may be helpful in observing seismo-ionospheric perturbations as a localized phenomena, as wavelets analysis give time and frequency localization in the given data. The discontinuities in STEC are also good in agreement with the energy and phase of the signals.

V. ACKNOWLEDGEMENTS

I sincerely acknowledge my heartfelt thanks to "Department of Science and Technology", India for funding this project.

REFERENCES

[1] Darcy Karakelian, Simon L. Klemperer, Antony C. Fraser-Smith, and Gregory C. Beroza, "A Transportable System for Monitoring Ultra Low Frequency Electromagnetic Signals Associated with Earthquakes", Seismological Research Letters Volume 71, Number 4, 423-436 July/August 2000

[2] V.V. Hegai [a,*], V.P. Kim [a], J.Y. Liu [b], "The ionospheric effect of atmospheric gravity waves excited prior to strong earthquake", Advances in Space Research 37 (2006) 653–659

[3] Tadahiko Ogawa[1], Nozomu Nishitani[2], Takuya Tsugawa[1], and Kazuo Shiokawa[2], "Giant ionospheric disturbances observed with the SuperDARN Hokkaido HF radar and GPS network after the 2011 Tohoku earthquake", *Earth Planets Space*, 64, 1295–1307, 2012

[4] Li-ming He [1], Li-xin Wu [1, 2], "Seismo-ionospheric Anomaly Analysis Method Based on Integrated Wavelet Transform", International Workshop on Earthquake Anomaly Recognition (IWEAR2011) Northeastern University, Shenyang, China

[5] Gwal A.K., Shaheen Rubeena, Panda Gopal and Jain Kumar Santosh, "Study of Seismic Precursors by Wavelet Analysis", *Research Journal of Engineering Sciences,* ISSN 2278 – 9472Vol. 1(4), 48-52, October (2012)

[6] Michael E. Contadakis[1], Dimitrios N. Arabelos[1], Christos Pikridas[1], Spyrous D. Spatalas[1], "Total electron content variations over southern Europe before and during the M 6.3 Abruzzo earthquake of April 6, 2009", Special Issue: Earthquake Precursors, ANNALS OF GEOPHYSICS, 55, 1, 2012; doi: 10.4401/ag-5322

[7] A. K. Singh,[1] Devendraa Siingh,[2] R. P. Singh,[3] and SandhyaMishra[1], "Electrodynamical Coupling of Earth's Atmosphere and Ionosphere: An Overview", International Journal of Geophysics Volume 2011, Article ID 971302, 13 pages doi:10.1155/2011/971302

[8] V.M. Sorokin *, V.M. Chmyrev, A.K. Yaschenko, "Electrodynamic model of the lower atmosphere and the ionosphere coupling", Journal of Atmospheric and Solar-Terrestrial Physics 63 (2001) 1681–1691

[9] Sergey Pulinets[1],* , "Ionospheric Precursors of Earthquakes; Recent Advances in Theoryand Practical Applications", TAO, Vol. 15, No. 3, 413-435, September 2004

[10] J. Y. Liu[1,2], Y. J. Chuo[3], S. J. Shan[1], Y. B. Tsai[4], Y. I. Chen[5], S. A. Pulinets[6], and S. B. Yu[7], "Pre-earthquake ionospheric anomalies registered by continuous GPS TEC measurements" Annales Geophysicae (2004) 22: 1585–1593 SRef-ID: 1432-0576/ag/2004-22-1585 © European Geosciences Union 2004

[11] O. Molchanov[1], E. Fedorov[1], A. Schekotov[1], E. Gordeev[2], V. Chebrov[3], V. Surkov1, A. Rozhnoi[1], S. Andreevsky[1], D. Iudin[4], S. Yunga[3], A. Lutikov[3], M. Hayakawa[5], and P. F. Biagi[6], "Lithosphere-atmosphere-ionosphere coupling as governing mechanism for preseismic short-term events in atmosphere and ionosphere" , Natural Hazards and Earth System Sciences (2004) 4: 757–767.

[12] Harrison, R.G, Aplin, K. and Rycroft, M.(2010), " Atmospheric electricity coupling between earthquake regions and the ionosphere", Journal of Atmospheric and Solar-Terrestrial Physics, 72(5-6). 376-381.ISSN 1364-6826 doi: 10.1016/j.jastp.2009.12.004.

[13] Y. Omori[1], Y. Yasuoka[2], H. Nagahama[1], Y. Kawada1,[3], T. Ishikawa[4], S. Tokonami[4], and M. Shinogi[2] , "Anomalous radon emanation linked to preseismic electromagnetic phenomena", Nat. Hazards Earth Syst. Sci., 7, 629–635, 2007.

[14] Surinder Singh[1, *], Arvind Kumar[1], Bikramjit Singh Bajwa[1], Sandeep Mahajan[1], Vinod Kumar[1], and Sunil Dhar [2], " Radon Monitoring in Soil Gas and Ground Water for Earthquake Prediction Studies in North West Himalayas, India", Terr. Atmos. Ocean. Sci., Vol. 21, No. 4, 685-695, August 2010.

[15] M. Matsumura[1], A. Saito[1], T. Iyemori[2], H. Shinagawa[3], T. Tsugawa[3], Y. Otsuka[4], M. Nishioka[4], and C. H. Chen[1], "Numerical simulations of atmospheric waves excited by the 2011 off the Pacific coast of Tohoku Earthquake", *Earth Planets Space*, 63, 885–889, 2011.

[16] V.V. Hegai [a,*], V.P. Kim [a], J.Y. Liu [b], "The ionospheric effect of atmospheric gravity waves excited prior to strong earthquake", Advances in Space Research 37 (2006) 653–659.

[17] Mokhamad Nur Cahyadi[1,2,*] and K. Heki[1], "Ionospheric disturbances of the 2007 Bengkulu and the 2005 Nias earthquakes, Sumatra, observed with a regional GPS network", Journal Of Geophysical Research: Space Physics, VOL. 118, 1777–1787, doi:10.1002/jgra.50208, 2013

